ANTIMONY ISOTOPES AS INDICATORS OF REDOX REACTIONS IN AQUEOUS SYSTEMS: FRACTIONATION DURING SB(V) REDUCTION BY SULFIDE AND ISOTOPE EXCHANGE KINETICS BETWEEN DISSOLVED SB(III) AND SB(V)

BY

JOEL STEPHEN MACKINNEY

THESIS

Submitted in partial fulfillment of the requirements
for the degree of Master of Science in Geology
in the Graduate College of the
University of Illinois at Urbana-Champaign, 2016

Urbana, Illinois

Adviser:

Professor Thomas M. Johnson

ABSTRACT

Antimony (Sb) has a history of being overlooked as an aqueous contaminant. The widespread commercial use of Sb has caused scientists to realize the importance of studying the fate and transport of Sb. For other contaminant elements, stable isotopic ratio measurements have been useful for source tracing and detection of environmentally critical chemical reactions (e.g., Wiederhold 2015). We seek to develop Sb isotopic ratios as tools for detecting and quantifying Sb in the environment. Currently, processes that generate shifts in ^{123}Sb/^{121}Sb are not well studied, though they can be inferred from theory and the isotopic systematics of other elements. To provide a more precise understanding of the drivers of Sb isotope variation, the magnitude of isotopic fractionation for individual reactions must be determined. In this study, we determine the magnitude of isotopic fractionation in environmentally relevant reactions. We use anion exchange resin and hydride generation MC-ICP-MS methods to obtain precise measurements of ^{123}Sb/^{121}Sb. The anion exchange method is also effective for separating Sb(III) from Sb(V).

First, we find that isotopic exchange between aqueous Sb(V) and Sb(III) at higher than natural concentrations (3 mM Sb) is negligible over a timescale of 6 weeks. At the lower concentrations of natural systems, exchange is likely to be much slower. Accordingly, we conclude that kinetic isotope effects that occur during Sb redox reactions are not overprinted by isotopic exchange, which would drive coexisting Sb(III) and Sb(V) toward isotopic equilibrium. Second, we quantified isotopic fractionation during reduction of 8.2 μM aqueous Sb(V) by sulfide to form amorphous Sb_2S_3. The data mostly conform to a Rayleigh distillation model, with 5 out of 11 data points deviating from the model slightly more than the measurement uncertainty. During experimentation it was found that the dissolved portion contained about 75% Sb(V) and

25% Sb(III). The best-fit model corresponds to an isotopic fractionation factor of 0.9986; Sb_2S_3 product was lower in $^{123}Sb/^{121}Sb$, relative to the dissolved portion. This is a larger magnitude of $^{123}Sb/^{121}Sb$ shift during Sb(V) reduction than observed by Rouxel et. al. (2003).

ACKNOWLEDGMENTS

I would first like to express gratitude to my adviser, Dr. Tom Johnson, for his advice, insight and always being available to answer my questions. He devoted a large sum of time, often into the late hours of the night, to help me complete this work. Thanks to Dr. Craig Lundstrom for being a supportive teacher throughout my time here and for editing my writing. I want to thank Dr. Gideon Bartov for being instrumental in helping me solve lab related questions. The friendship of the graduate students I worked alongside in the lab and office is much appreciated: Naomi Wasserman, Noah Jemison, Matt Bizjack, Nicole Fernandez, Zhenhao Zhou, Max Giannetta, Yuchen Liu and Xiaobao Lin. Thank you to my family, Ted, Rachel, Erin and Ben, for your unwavering support and always being quick to encourage and affirm.

TABLE OF CONTENTS

CHAPTER 1- INTRODUCTION

Antimony (Sb) is very common in modern consumer products but frequently overlooked despite its toxicity. Sb is added in low quantities to diverse products from brake pads and ammunition to flame resistant cloths and plastic water bottles (Anderson 2012). It poses little risk in these products, but high concentrations of this element in drinking water can be detrimental to health (Poon et. al. 1998). Plants can become contaminated by uptake from roots or by settling atmospheric dust (Shotyk et. al. 2005b). Highly contaminated sites do not often occur naturally but commonly result from Sb mining and ore extraction. Background concentrations in water are usually less than 9 nM (Filella et. al. 2002), but streams, lakes, and rivers around Sb or other mine sites can have highly elevated concentrations. A mine-polluted river in China was found to have 241 µM Sb (He et. al. 2012); about 5,000 times higher than the 49 nM limit for drinking water set by the United States of America Environmental Protection Agency (USA- EPA). Since there is large commercial demand for Sb (Anderson 2012), contaminated systems are increasingly common around the world (Shotyk et. al. 2005a; Amarasiriwardena and Wu 2011; He et. al. 2012). Thus there is an urgent need to study the aqueous geochemistry of Sb for ecological and remediation purposes.

While awareness and research for Sb is accelerating, knowledge of Sb geochemistry is still less than for other elements such as arsenic (As). Out of nescience, Sb is often compared with arsenic (As). While the two are similar in toxicity and oxidation state, it is a mistake to assume that their geochemistry is the same in aqueous environments. The relevant oxidation states for Sb and As in most natural conditions are +III and +V. Sb(V) often appears more mobile in surface waters while Sb(III) tends to adsorb and precipitate more readily (e.g., Ritchie et. al. 2013). This relationship is opposite to observations of As, for which greatest problems for drinking water is As(III) in groundwater wells (Smedley and Kinniburgh 2002).

For “pure” waters (pH 6-8.5) with low concentrations of major anions, Sb is reported to exist as antimonate ($Sb(OH)_6^-$) or antimonite ($Sb(OH)_3$) depending on water chemistry and reducing potential (Eh). Sb-chloride and Sb-sulfide species are both important in nature. Filella et. al. (2002) provides a more extensive review of Sb species in natural waters.

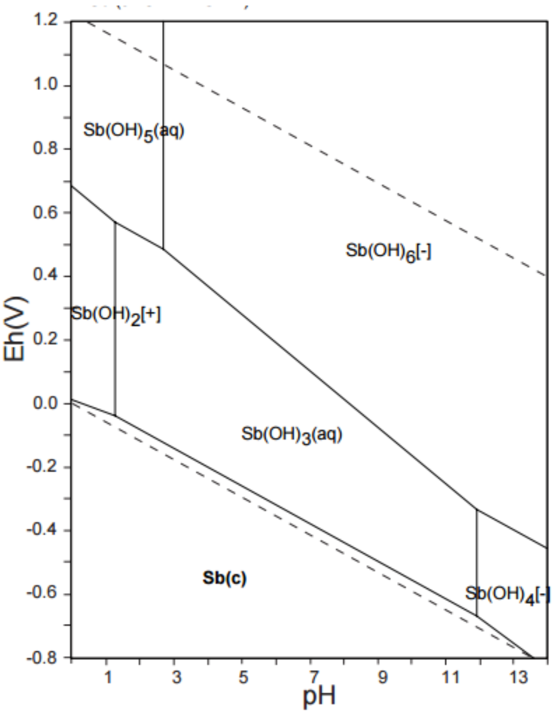

Fig. 1: Pourbaix diagram for Sb-O-H system at [10^{-10}] Sb, 298.15K, 105 Pa (Takeno 2005).

In oxidizing conditions $Sb(OH)_6^-$ is the more stable form and this oxidation state has been found to dominate in most surface waters (Ritchie et. al. 2013; Resongles et. al. 2015), but there are significant exceptions to this (Filella et. al. 2002). Sb commonly participates in adsorption reactions, especially with Mn, Al and Fe (oxy)hydroxides and natural organic matter (Pilarski et. al. 1995; Thanabalasingam and Pickering 1990; Leuz, Mönch and Johnson 2006; Ilgen and Trainor 2011; Ritchie et. al. 2013; Buschmann et. al. 2005). Both Sb(V) and Sb(III) will adsorb onto surfaces, with less adsorption as the pH of water increases. Sb(III) adsorbs in a wider range of conditions than Sb(V) (Leuz et. al. 2006).

The persistence of Sb in solution depends highly on the geochemical components of the environment (e.g., Wilson et. al. 2012). Natural remediation may occur by precipitation of sulfide minerals in sulfidic reducing conditions (Wilson et. al. 2012) or by adsorption onto various surfaces (Thanabalasingam and Pickering 1990). Water treatment methods have greater removal efficiency for Sb(III) compared to Sb(V) (Guo et. al. 2009). One paper indicated the possibility of remediation of Sb mine drainage by Sb(V) reduction with sulfide (Wang et. al. 2013). Because of this, it is important for research to be able to distinguish between oxidation states. In their review, Ungureanu et. al. (2015) stress the importance of remediation of Sb as a rising contaminant. There is a need to develop methods to monitor the long term efficacy of natural and artificial remediation.

Conventional monitoring of remediation is performed by measuring the total concentration of Sb in the aqueous phase. This strategy has the merit of cost effectiveness, but can sometimes lead to the erroneous recognition of remediation when another physical process has occurred. In a surface or groundwater setting, advection, dispersion and adsorption will spread and redistribute dissolved Sb. This may cause a decrease in concentration without reducing overall contaminant mass. A more comprehensive approach to monitoring should include some way of identifying change in oxidation state and specific chemical pathway.

Isotopic studies are an emerging approach to gaining useful information on particular contaminant elements in a system (Wiederhold 2015). Little work has been done to develop Sb isotope measurements; here we seek to expand our knowledge by applying isotopic methods that have been successful for other elements such as chromium (e.g., Berna et. al. 2009). Sb has two stable isotopes, ^{121}Sb and ^{123}Sb, with average abundances reported as 57.21% and 42.79%, respectively (Berglund and Wieser 2011). The isotopes are not chemically identical and thus some chemical reactions can cause a measurable change in the $^{123}Sb/^{121}Sb$ ratio. These shifts in the isotopic ratio are known as isotopic fractionation. As Johnson (2012) presented, isotope-based studies are challenging because of the ubiquitous complexity found in nature and the very high measurement precision required, but isotope ratio measurements can serve as powerful indicators of chemical processes such as reduction.

The magnitude of variation in the $^{123}Sb/^{121}Sb$ ratio is very small, so notation has been developed to more easily report and compare the values. Variations are expressed as $\delta^{123}Sb$, a relative difference between a measured $^{123}Sb/^{121}Sb$ ratio and that of a standard:

$$\delta^{123}Sb = (R_{sample} / R_{standard} - 1) * 1000‰ \qquad (1)$$

where R represents the isotopic ratio $[^{123}Sb] / [^{121}Sb]$. $\delta^{123}Sb$ is commonly expressed as a permil (‰) quantity because variations are small. A positive value of $\delta^{123}Sb$ indicates enrichment of a sample in ^{123}Sb relative to the standard, whereas a negative value indicates depletion of ^{123}Sb. The standard used in our study is AOA312974, an in-house solution created from Sb_2O_3 (Acros Organics, CAS 1309-64-4, lot AO312974).

Certain chemical reactions can fractionate Sb isotopes; the reaction product's $\delta^{123}Sb$ differs from that of the reactant. The direction and magnitude of fractionation (i.e., the isotopic difference in ^{123}Sb / ^{121}Sb between the reactant and product) of a reaction is expressed as a fractionation factor, α:

$$\alpha = [^{123}Sb / ^{121}Sb]_{product} / [^{123}Sb / ^{121}Sb]_{reactant} \qquad (2)$$

α is usually very close to unity and is somewhat awkward in common use. Because of this, kinetic isotopic fractionation, the shift in the isotopic ratio produced by a kinetic reaction (e.g., Sb reduction), is conveniently expressed as a per mil deviation of α from unity, ε:

$$\varepsilon = (\alpha-1) * 1000‰ \approx \delta^{123}Sb_{product} - \delta^{123}Sb_{reactant} \qquad (3)$$

In this study, we consider two types of mass-dependent isotope fractionation: equilibrium and kinetic. Equilibrium fractionation stems from slight differences in the thermodynamic properties of the two isotopes, and can be explained by the concept of zero point energy in quantum mechanics. The total energy of a system is usually lowered when the heavier isotope (^{123}Sb) is at a higher oxidation state (Sb(V)) (Schauble 2004). In an aqueous system containing Sb(III) and Sb(V), if isotopic equilibrium is approached, the Sb(V) species will be enriched in ^{123}Sb relative to the Sb(III) species. If Sb isotopes are exchanged rapidly between the two valence states, Sb(V) and Sb(III) could evolve rapidly toward isotopic equilibrium. With Fe, isotopic exchange can be rapid and drive coexisting Fe(III) and Fe(II) species to isotopic equilibrium (Johnson et. al. 2002; Anbar et. al. 2000).

At the outset of this study we hypothesized that the isotopic exchange rate, and thus the rate of approach toward isotopic equilibrium is similar to the very slow rates observed for Cr and U (Wang et. al. 2015a; Wang et. al. 2015b). For U, Cr, and Sb, multiple electrons must be exchanged and bond coordination changes; both decrease the rate of exchange. In this case, the progression toward isotopic equilibrium between Sb(III) and Sb(V) in solution would be negligible for most natural conditions and reactions. This research includes the first experiments to determine if Sb isotopic equilibrium is rapidly established between Sb(III) and Sb(V).

Kinetic fractionation results from the greater reaction rate of the lighter isotope. The two-neutron mass difference between ^{121}Sb and ^{123}Sb slightly affects the effective activation energy of reactions, and depending on the type of reaction, one isotope will react at a greater rate relative to the other. The largest isotopic fractionation is induced when the change in bond coordination and strength is greatest (Schauble 2004). Based on past experience with S, Se, Cr, U, and Hg, reduction reactions typically produce larger isotopic fractionation than other reactions; we expect reduction of Sb(V) to Sb(III) to follow this pattern. Only two laboratory experiments of Sb isotopic fractionation have been published to date; there is a need to supplement the modicum of relevant experiments.

The earliest publication examining Sb isotope variation reported fractionation during the reduction of Sb(V) to Sb(III) by potassium iodide (Rouxel et. al. 2003). They obtained fractionation factors (ε) of -0.55‰ and -0.9‰ for two experiments with different conditions. A more recent meeting abstract (Araki et. al. 2009) reported a slight enrichment of ^{123}Sb in the aqueous phase as Sb(V) adsorbed onto synthetic ferrihydrite. However, the magnitude was not reported.

Several studies have examined natural variations in δ^{123}Sb in a variety of geochemical environments (Resongles et. al. 2015; Lobo et. al. 2012; Lobo et. al. 2013; Lobo et. al. 2014; Tanimizu et. al. 2011; Asaoka et. al. 2011; Rouxel et. al. 2003). Unfortunately, as Resongles and colleagues (2015) point out, we cannot directly compare results from different studies due to different internal standards used in each case. Measurements within a study can be compared and thus give an overall magnitude of variation for a process but comparison between studies remains difficult.

The most common Sb ore is the sulfide (Sb_2S_3). In its crystalline form it is a silvery grey mineral, stibnite, while the amorphous form, metastibnite, is bright orange. Because Sb is so commonly associated with sulfur, most current Sb isotope work has examined δ^{123}Sb variations related to Sb sulfides directly (stibnite) or indirectly (mine impacted water). Lobo et al. (2012) observed a variation spanning 1‰ in stibnites from Spain, Romania, The United States of America, and China. Each country had a unique range of δ^{123}Sb, such that it could be possible to distinguish between stibnite ores from different locations. Another study compared stibnite ore to mine drainage water in Japan (Tanimizu et. al. 2011). The mine water was enriched in ^{123}Sb by 0.35‰ compared to the stibnite. The reason for this difference is unclear, but the authors suggest it could be due to sequential adsorption of $Sb(OH)_6^-$ onto Fe hydroxides based on the research from Araki et. al. (2009). A third study measured δ^{123}Sb for various seafloor hydrothermal sulfides (Rouxel et. al. 2003). They found a variation of 1.8‰ among different locations. Their data support the idea that Sb(V) was reduced to form stibnite at hydrothermal vents. This reduction preferentially enriches the remaining fluid in δ^{123}Sb; this fractionation could cause the significant isotopic variation observed.

Most recently, several authors examined the progression of δ^{123}Sb from mine sources to downstream in two mine-affected watersheds in southern France (Resongles et. al. 2015). Isotopic composition differed in the two watersheds with a range of -0.06‰ to +0.11‰ in the upper Orb River and +0.23‰ to +0.83‰ in the Gardon River watershed. Little change in δ^{123}Sb was observed in a downstream progression. The authors attributed this to conservative transport of Sb(V) based on the river geochemistry (near neutral pH, <50 μg/L Fe and <1 mg/L organic matter).

Experiments determining the magnitude and direction of Sb isotopic fractionation for relevant natural reaction (adsorption, oxidation, and reduction) are currently needed and would promote more accurate interpretation in field studies like those summarized above. In this study we present controlled laboratory experiments determining Sb isotopic fractionation for environmentally relevant reactions. We refine previously established methods for sample preparation, Sb(III)-Sb(V) separation, and ^{123}Sb / ^{121}Sb ratio measurement to obtain highly precise and accurate data. We present the first determination of the rate of isotopic exchange between Sb(III) and Sb(V) in solution and the first determination of Sb isotope fractionation during reduction of aqueous Sb(V) by sulfide to form metastibnite. This experiment will aid in interpretation of both the large range of δ^{123}Sb found in natural stibnite samples (Lobo et. al. 2012) and among hydrothermal sulfides (Rouxel et. al. 2003). It will also enable Sb isotope studies to monitor Sb remediation via stibnite deposition at contaminated sites (e.g., Wilson et. al. 2012). In summary, the experiments I present seek to further our understanding of isotopic behavior in key geochemical settings so Sb isotopes can be used to track natural Sb redox reactions.

CHAPTER 2- MATERIALS AND METHODS

2.1 Reagents

All solutions used water purified with a Millipore Milli-Q 18 MΩ-cm deionizing system. Distilled hydrochloric acid was used for chemical separation and sample preparation. Teflon © (PTFE) beakers, separation columns and glassware were cleaned in a three step procedure using soap, 8 M reagent grade nitric acid, and 6 M reagent grade hydrochloric acid. Equipment was soaked overnight in each solution and rinsed three times with ultrapure water. Experiment vessels were wrapped in aluminum foil to prevent any possible photochemical reactions. Sodium borohydride solution at 0.2% (m/v) was prepared fresh daily for use in hydride generation, and stabilized in 0.2% (m/v) sodium hydroxide. The Sb(V)-reducing solution (0.3 M KI and 0.28 M L-ascorbic acid) was prepared by mixing 5.0 g of potassium iodide (Fisher chemical) and 5.0 g of L-ascorbic acid (Fisher chemical) in 100mL of water. A 1.7 μM Sb stock solution was created from Sb_2O_3(s) (Acros organics) with 2 M distilled HCl. The 8 nM bracketing standard (AOA312974) was prepared from the concentrated solution every two weeks in 0.05% (m/v) reducing solution and 2 M HCl. Asaoka et. al. (2011) suggest 3 hours be given for 98% reduction of Sb(V) to Sb(III) in 0.5% KI-ascorbic reducing solution. A 1.87 mM Sb(V) stock solution was created by diluting 99% anhydrous $SbCl_5$ (CAS 7647-18-9, LOT AO307008) with 1 M HCl. A third solution used was a 1000 mg/L $SbCl_3$ reference solution (Fisher Chemical) that was diluted as needed. While Sb(V) is stable in a variety of conditions, Sb(III) will oxidize over time. As such, Sb solutions without reducing solution added have limited stability. Stability of Sb(III) solutions varies, depending on matrix and exposure to oxygen.

2.2 Sulfide reduction experiment

The goal of this experiment was to determine the magnitude of isotopic fractionation as Sb(V) is reduced by sulfide and precipitated as solid Sb_2S_3. The element must undergo significant bond changes as Sb(V) is first reduced to Sb(III) and then bound to sulfur. A 51.3 μM sulfide solution was made by dissolving $Na_2S.9H_2O$ in water; fresh batches of this stock were created immediately before use. Anoxic serum bottles with thick blue butyl rubber stoppers were used as reaction vessels. All bottles and solutions were purged with nitrogen (N_2) for at least one hour prior to use. Syringes were purged with N_2 prior to, and N_2 was always injected before, extraction of samples from serum bottles, to keep positive pressure inside. Varying extents of Sb(V) reduction were induced in a series of six identical serum bottles containing 8.2 μM Sb(V) by injecting varying volumes of the sulfide stock solution. The experiment matrix was 0.5 M HCl. Total volume of solution was approximately 35 mL and the serum bottle has a maximum volume of 125 mL. To prevent the experiment from being diffusion limited (see discussion), each bottle was stirred vigorously with a Teflon-coated stir bar during sulfide addition to ensure rapid homogenization.

After 20 days, the Sb_2S_3 solid was separated from the liquid with a 0.22 μm polyethersulfone filter (Millex-MP Filter Unit with Millipore Express Membrane). Filtrate was put into clean glass tubes. Some precipitate was found clinging to the Teflon stir bars. Serum bottles were opened and separation was done as quickly as possible to reduce exposure time to oxygen. Stir bars and filter papers were rinsed thoroughly with ultra-pure water to remove remaining solution. The precipitate was dissolved from each filter paper and stir bar by soaking overnight in 6 M HCl.

2.3 Isotopic exchange rate experiment

The purpose of this experiment was to determine the rate of Sb isotopic exchange between Sb(III) and Sb(V) in solution. An anoxic and aluminum foil-coated 125 mL capacity serum bottle was used as a reaction vessel. About 11 mL of a solution containing approximately equal portions of Sb(III) and Sb(V) with an overall Sb concentration of 3 mM was created in a serum bottle. The experiment was performed in 1.0 ± 0.1 M HCl. Sb(V) was obtained from the stock solution of $SbCl_5$ and Sb(III) was diluted from the Fisher $SbCl_3$ reference solution. The experiment was designed to have extremely high Sb(V) and Sb(III) concentrations to increase rate of interaction between Sb atoms and thus rapid exchange (see discussion). The bottle was kept at a constant 21^oC. The $\delta^{123}Sb$ of each solution was measured before mixing. Samples were collected at different intervals (0, 2, 4, 9, and 80 days) and diluted to 16.5 μM Sb before separation of Sb(III) from Sb(V).

2.4 Reproducibility of $\delta^{123}Sb$

Reproducibility of the measurement methods was demonstrated by multiple measurements of Sb extracted from a high matrix sample. One sample of coal fly ash from the Tennessee Valley Authority’s Power Plant at Kingston, Tennessee, USA was subjected to two separate digests in aqua regia. A small fraction of silica and other materials that did not digest were discarded. Sb dissolves readily in this solution and so Sb recovery was thought to be quantitative. Samples were diluted to 1 μg / L and measured with and without the anion exchange matrix removal method.

2.5 Anion exchange and speciation

In previous studies, thiol-cotton fiber (TCF) and thiol-cellulose powder (TCP) were commonly used for purification (Rouxel et. al. 2003; Tanimizu et. al. 2011; Resongles et. al. 2015). TCF and TCP are advantageous because they remove Te from samples. However TCF is time consuming to prepare and has a limited working life span. Instead, we used an anion exchange procedure modified after Łukaszczyk and Żyrnicki (2010) combined with a Te correction performed during isotope analysis. The Te correction was shown to be acceptable up to 1:1 Te:Sb (see section 2.10.1). In the event of higher Te concentrations, one of the previous Te separation procedures using TCF or TCP could be used.

In chloride form, anion exchange resin can be used to separate Sb(III) from Sb(V) (Łukaszczyk and Żyrnicki, 2010). The sorption of Sb(III) is quantitative in the range of 1.0 to 2.0 M HCl. At 1.5 M HCl, Sb(III) is retained in the resin as $SbCl_6^{3-}$ and $SbCl_4^-$, while Sb(V) passes through as the neutral species, $Sb(OH)_xCl_{(5-x)}^0(aq)$.

Ion exchange columns (Bio Rad® polyprep with 2ml resin volume) were filled with 1.4 mL of AG 1 x 8 (100-200 mesh) chloride form anion exchange resin (Eichrom®) consisting of styrene divinyl benzene polymeric beads with quaternary amine functional groups. New resin is cleaned with Methanol, 1.0 M NaOH, and 1.0 M HCl. 15 mL of 1.5 M HCl is used to pre-condition resin before sample addition.

The resin can also be used to separate Sb from most other solutes. The KI reducing solution can be used to completely reduce total Sb to Sb(III). In a 1.5 M HCl matrix, Sb(III) binds to the resin while most matrix components are eluted. Sb(III) is recovered by elution with water or weak acid. An important note for this procedure is that iodine from the reducing solution binds strongly to the resin such that new resin must be used each time this procedure is performed. If too much KI reducing solution is used the resin becomes loaded with KI and loses its capacity to bind Sb(III). Avoid adding more than 0.1 mmoles of strongly adsorbing species such as iodine to the column.

Tests were performed to prove the efficacy of the anion exchange procedure. We have shown that recovery is quantitative. Sb(V) is eluted immediately as HCl is added, while Sb(III) does not elute until after the eluent is changed to water. The two species are clearly separated (Fig. 2). No special measures were needed to avoid oxidation of Sb(III) to Sb(V). Tests were performed to show that columns can be performed in regular atmosphere. Slow oxidation rate of Sb(III) was also suggested by Leuz and Johnson (2005). It is good to run samples (without KI reducing solution) through column within ~2 hours of exposure to oxygen. Sb(III) samples with reducing solution present are stable for at least several days. Column recovery was tested using a sample of coal fly ash (KFA) that was digested in aqua regia. After digestion, all Sb is likely found as Sb(V). This Sb was reduced to Sb(III) with KI reducing solution and added to the columns. Recovery was found to be 100.5% ± 1.6% (1 stddev).

An important discovery is that significant artificial isotope fractionation occurs in both the Sb(V) and Sb(III) in the columns (Fig. 2). This does not induce an overall artificial fractionation of the eluted sample as long as Sb recovery is close to 100%. It was originally thought that Sb(V) passes through the column without interaction with the resin, however the observed isotopic fractionation indicates that some Sb(V) interaction with the quaternary amine functional groups takes place. This fractionation could be explained if some of the Sb(V)-chloride complexes are charged or polar species. This suggests that not all the Sb(V) is a neutral complex as suggested earlier (Łukaszczyk and Żyrnicki 2010).

The first Sb that elutes in the Sb(III) portion is enriched in ^{123}Sb (Fig. 2), which indicates that ^{121}Sb is retained more strongly on the resin. A mechanism for this could be kinetic isotopic fractionation between Sb-Cl species. It is reported that Sb(III) exists as $SbCl_6^{3-}$ and $SbCl_4^{-}$ (Łukaszczyk and Żyrnicki 2010). An Sb Chloro-complex with more chlorine bonds ($SbCl_6^{3-}$)

should be enriched in ^{121}Sb relative to those with less chlorine atoms attached ($SbCl_4^-$). Thus the ^{123}Sb-chloro complexes, having fewer chlorine atoms attached, would elute before the ^{121}Sb-chloro complexes. A similar effect was shown for Fe chloro-complexes on ion-exchange columns (Anbar et. al. 2000). Thus it is imperative to quantitatively recover the entire intended Sb species peak or column artifact could occur.

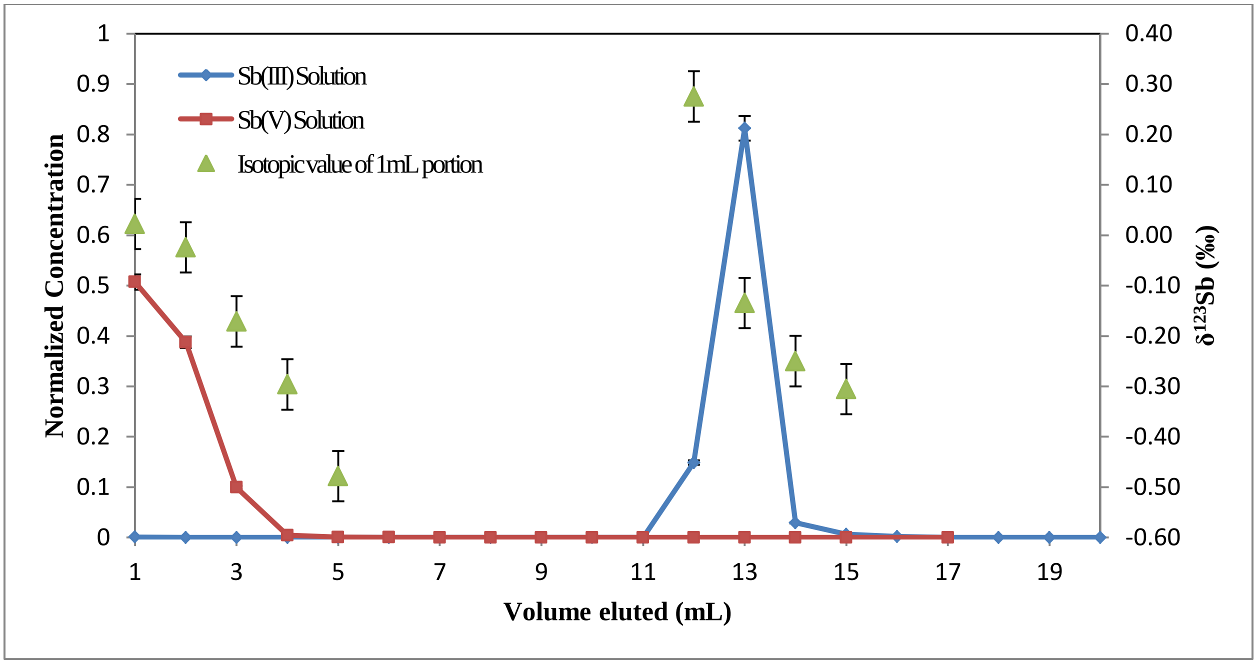

Fig. 2: Normalized concentration and δ^{123}Sb for one Sb(III) solution and one Sb(V) solution processed using the anion exchange protocol described above. Points represent compositions of successive 1.0 mL volumes eluted. Eluent was 1.5 M HCl for 1 to 10 mL and H_2O for 11 to 20 mL is H_2O. Concentration and δ^{123}Sb were measured for each 1.0 mL portion.

2.6 Concentration measurement

Sb concentrations were measured on a Thermo Scientific™ iCAP™ Q ICP-MS at the University of Illinois at Urbana-Champaign before isotopic measurement. Samples were diluted to <0.41 μM Sb in 2% HNO_3. A standard calibration curve was created with a blank and four standard concentration solutions (0 μM, 0.041 μM, 0.2 μM, 0.41 μM, and 0.82 μM). Indium (^{115}In) was used as an internal standard to improve precision of measurements. ^{115}In was continually mixed into samples with an extra channel on the peristaltic pump. In addition, a collision cell was used to reduce interference from the matrix. Polyatomic interferences are suppressed by inputting a reactive gas (He) combined with Kinetic Energy Discrimination (KED). Background equivalent concentration (BEC) was 4 ng/L. The limit of detection (LOD) was 1.0 ng/L and the relative standard error of the calibration curve was 0.722%. Precision was estimated on duplicate measurements. One sample measurement was 420 ± 10 μg/L Sb (2σ). These measurements were used to dilute samples for isotopic measurement.

2.7 Hydride generation

Hydride generation (HG) is an effective means to volatilize Sb for measurement (Dedina and Tsalev 1995) and increases sensitivity by separating Sb from the matrix allowing very low Sb concentration solutions to be measured precisely and accurately for isotope ratio. This is important since most natural waters are less than 1 μg/L (8.2 nM). Methods that use conventional nebulizers or even desolvating nebulizers are not practical for natural aqueous Sb samples, because of the high Sb concentration required. HG allows for accurate measurement of concentrations down to 4 nM and of isotopic ratios down to 1.5 ng per 3 ml sample acquisition.

Hydride generation is highly selective for Sb(III). Signal intensity is 15 times higher for Sb(III) compared to Sb(V) (Table 1). Sb(III) is reduced to H_3Sb faster and with higher chemical yield than Sb(V) (Dedina and Tsalev 1995). Incomplete H_3Sb formation takes place when Sb is present as Sb(V), inducing a -0.5‰ artificial fractionation (Table 1).

Table 1. Comparison of the Sb(V) bracketing standard with and without reducing solution

8.2 nM AOA312974	Intensity ^{121}Sb (Volts)	δ^{123}Sb (‰)
KI reducing solution added	4.655	NA*
	4.646	NA
	4.661	NA
No reducing agents	0.298	-0.34
	0.291	-0.54
	0.292	-0.52

*δ^{123}Sb for bracketing standard is NA because this value is defined as "0"

Because Sb(V) is not suitable for analysis, a reducing agent that can completely reduce Sb(V) to Sb(III) is needed. The commonly used mixture of potassium iodide and ascorbic acid was selected for the present study (Dedina and Tsalev 1995; Rouxel et. al. 2003; Tanimizu et. al. 2011; Asaoka et. al. 2011; Resongles et. al. 2015). Asaoka et. al. (2011) achieved >95% recovery with this mixture. KI acts as the primary reducing agent while ascorbic acid serves to stabilize the solution and aid in reduction. The efficacy of reduction was tested by taking an Sb(V) sample, reducing it with the KI reducing solution and then performing the speciation procedure. In this test, column recovery was 96.6% and it was found that 99.8% was Sb(III).

Another important factor in the HG is acidity. Dedina and Tsalev (1995) report that higher concentrations of acid provide a faster and more efficient pre-reduction of Sb(V) to Sb(III) by KI. All samples and standards were adjusted to 2 M HCl before measurement.

The hydride generation apparatus used in this study is similar to that described by Rouxel et. al. (2002). The main differences in the setup used here are no mixing coil, gas-liquid separator (GLS) at room temperature, and different reagent concentrations. The GLS used in this study was produced on site at the University of Illinois at Urbana-Champaign. A multi-channel peristaltic pump is used to control flow of sample, $NaBH_4$ and waste. Sample uptake is approximately 1 mL/min. Isotopic measurement is performed at approximately 8 nM Sb and requires about 3 mL of sample. The $NaBH_4$ and sample solution meet at a mixing junction constructed out of fluoropolymer plastics. The HG apparatus is rinsed for four minutes with reagent grade 2 M HCl between each measurement. The retention of residual Sb in the tubing is low and a four minute wash is more than adequate to bring Sb signal down to background levels.

2.8 Mass spectrometry

The difference in mass between ^{121}Sb and ^{123}Sb is 1.6%. Thus, isotope ratio variation is small (Schauble 2004), and very precise measurement techniques are needed. HG coupled to a multi-collector mass spectrometer fulfills this requirement. Sample analysis was performed on a Nu Plasma HR multi-collector inductively couple plasma mass spectrometer coupled to a continuous-flow hydride generation system (HG-MC-ICP-MS) at the University of Illinois at Urbana-Champaign. This measurement setup is similar to previous studies and is effective for ^{123}Sb/^{121}Sb measurement (Rouxel et. al. 2003; Resongles et. al. 2015). Faraday collector settings are outlined in table 2.

Table 2. Collector settings for ^{123}Sb/^{121}Sb measurement

L5	L4	L3	L2	Ax	H2	H4	H5	H6
NA	120	121	122	123	124	125	126	NA
NA	^{120}Sn ^{120}Te	**^{121}Sb**	^{122}Sn ^{122}Te	**^{123}Sb** ^{123}Te	^{124}Sn ^{124}Te	^{125}Te	^{126}Te	NA

The in-house bracketing standard named AOA312974 was used to correct for instrumental mass bias. This method entails alternating measurements of sample and standard. The sample δ^{123}Sb is reported compared to the average value of the two standards which “bracket” it. This mass bias correction method is also used by others (Rouxel et. al. 2003; Resongles et. al. 2015).

Because δ^{123}Sb values are reported relative to a specific standard, different studies cannot be directly compared unless the same standard was employed. As Resongles et. al. (2015) indicated, future Sb isotope studies should use the same standard so that Sb isotopic work can be unified. It is also necessary to establish secondary standards that have isotopic compositions far from that of the primary standard, to ensure measurements are accurate across a range of ^{123}Sb/^{121}Sb values. A fractionated standard (-0.82‰ relative to AOA312974) named FUCA15b was created by partially reducing a concentrated Sb(V) solution. FUCA15b was used to evaluate analytical accuracy and precision at the start of each session.

The standard-sample bracketing (SSB) method was found to be a suitable option using careful control of hydride generator settings and measuring each sample multiple times. External precision was determined to be 0.04‰ (2σ) using the method outlined in Wang et. al. (2015a). This value is based on uncertainty determined from duplicate sample preparations measured in the Sb(V) reduction experiment (±0.037‰ (n=4)) and the equilibrium experiment (±0.035‰ (n=8)). Procedural and chemical blanks are estimated to be 1.2% of typical sample mass based on running several blank samples through the column procedure using the same acids. In the Sb(V) reduction experiment, column blanks were 0.1% the concentration of samples on average.

Background correction was made for each sample using electrostatic analyzer (ESA) deflection with an integration time of 10 seconds. The ESA can deflect the ion beam away briefly, allowing the Faraday collectors to zero any remaining signal before sample measurement. Each isotope value was made in 3 blocks with 10 measurements per block and an integration time of 2 seconds per measurement.

During testing of the measurement protocol, it was found that as Sb concentration was decreased below 4 nM, δ^{123}Sb decreased (Fig. 3). Therefore, sample concentration should be between 0.5 and 1.5 ug/L (4 to 12 nM).

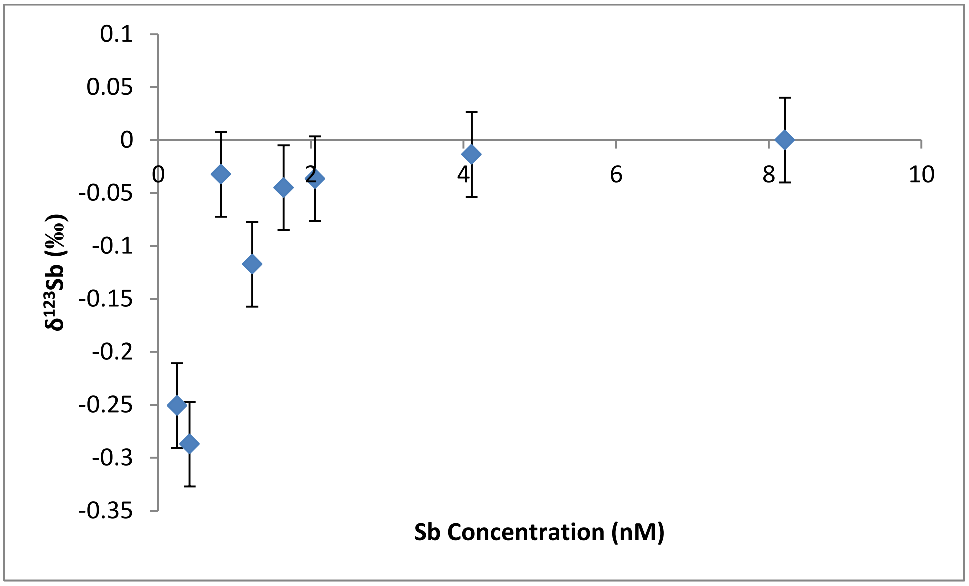

Fig. 3: δ^{123}Sb as a function of concentration. Created by dilution of the AOA312974 standard

2.9 Interferences and corrections

Hydride generation acts as a method of matrix removal because Sb is volatilized out of the sample and the bulk of the solution is drawn out as waste. Beside Sb there are many other elements that form volatile hydrides such as As, Ge, Bi, Te, Sn, Se and Hg. In many cases, interference from other hydride-forming elements and non-hydride forming matrix components are minor and not found to impact isotope values. However there are some important exceptions.

2.10.1 Tellurium interference

A correction was applied for the isobaric interference ^{123}Te. Most environmental samples contain very low concentrations of tellurium, and Te can be separated from Sb if necessary using TCF or TCP. However, because traces of Te occur in reagents and small amounts of Te may be present after Sb separation from sample matrices, a correction was applied to each measurement to account for the Te contribution to ^{123}Sb. This uses a mass bias-corrected ^{126}Te/^{123}Te value to calculate the intensity of ^{123}Te included in the total signal measured at mass 123. The mass bias exponent for the ^{126}Te/^{123}Te value comes from a relation between natural abundance of these isotopes compared to average ratios measured on the multi collected mass spectrometer. The calculated ^{123}Te intensity is then subtracted from the measured intensity at mass 123. This calculation is performed in real time via the data reduction software provided by the instrument manufacturer. ^{123}Te has an isotopic abundance of 0.89%, so the signal tends to be small. The method successfully corrected for Te even when standards were spiked with Te concentration equal to that of Sb (Fig. 4).

Several experiments were performed to test this Te correction. The tests revealed that the Te correction is successful and that the Te signal is greatly diminished by the reducing solution. The KI reducing solution used for all the Sb isotope analyses reduces Te(IV) to Te^0. However, the reduction rate of Te was slow and required a week for significant reduction to elemental Te. The elemental form of Te does not readily react with $NaBH_4$ to form a hydride. It also appears that when samples contain higher Te concentrations, a greater fraction is reduced to Te^0 as shown by the decrease in offset from the 0.5 Te:Sb ratio to 1 Te:Sb (Fig. 4). All Sb standards were spiked with varying amounts of Te six days before analysis.

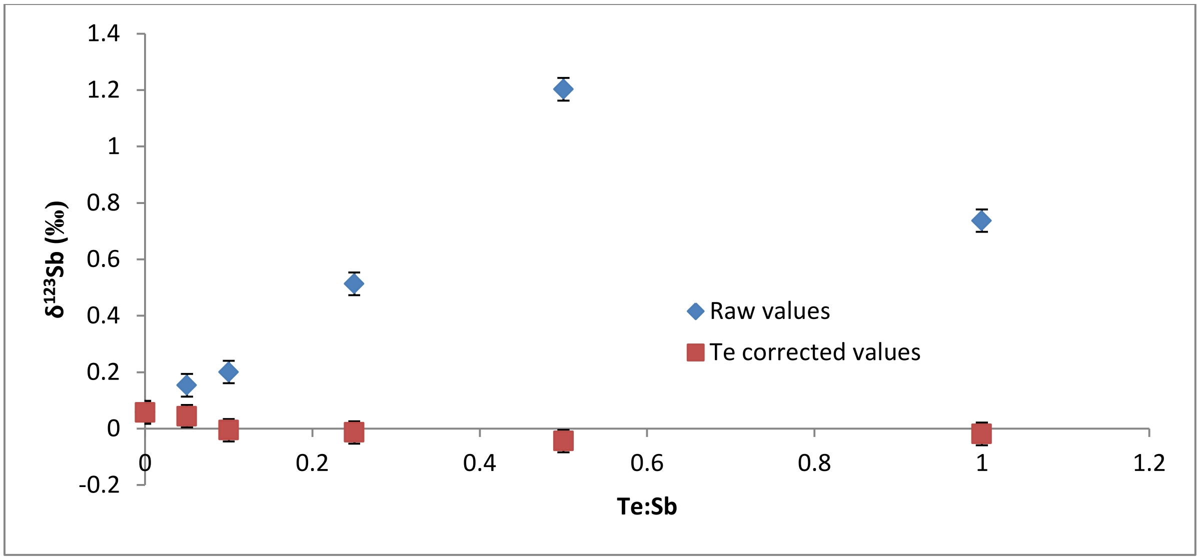

Fig. 4: δ^{123}Sb values of samples with varying amounts of Te added. 1 ug/L Sb samples were spiked with Te up to a 1:1 ratio. Significant artificial fractionation (blue diamond) is observed when no Te correction is applied, but corrected values (red squares) are near the value of the bracketing standard

2.10.2 Iron interference

Other authors have reported that high Fe(III) in an Sb sample can create artificial isotope fractionation (e.g. Rouxel et al., 2003). This is thought to occur because Fe(III) oxidizes Sb(III) back to Sb(V) or prevents Sb(V) reduction by KI. In the HG setup used for this study, it was discovered that Fe(III) affected the isotopic values of a 1 ug/L Sb standard solution only when Fe(III) concentration reached 318 mg/L. Perhaps the choice of reducing agent helps to accommodate the large Fe concentration before interference is observed (Näykki et. al. 2001). At 318 mg/L Fe, the solution is stained yellow; we thus suggest qualitatively that any samples that appear colorless should not be impacted by iron interference. This is the case for most natural waters.

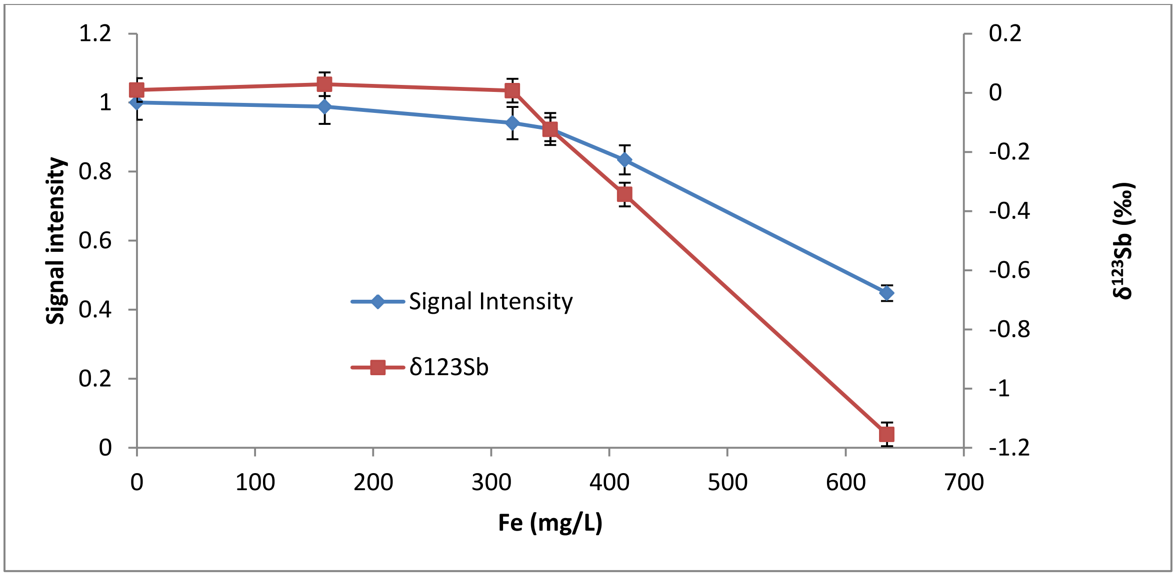

Fig. 5: Increasing concentrations of Fe(III) from $FeCl_3.6H_2O$ was added to samples of 1 ug/L Sb in 0.05% reducing solution. Concentration (blue diamonds) begins to decrease when Fe(III) overpowers the reducing agent and inhibits reduction of Sb(V) to Sb(III). Isotopes (red squares) begin to fractionate significantly after ~10% of original signal is lost.

2.10.3 Matrix Interference

Other tests were performed to determine if different sample matrices including synthetic groundwater (Table 3) and arsenic solutions impacted isotopic measurements. These did not impact the isotopic value of Sb. Even though As also readily forms a hydride, it was not found to influence Sb isotopic values. As a result we conclude that presence of hydride forming elements other than Te will not influence Sb isotopic composition, as other authors have reported (Rouxel et. al. 2003; Hall and Pelchat 1997).

Table 3. Concentration of solutes in synthetic groundwater

Species	Concentration (mM)
$NaHCO_3$	7.70
KCl	0.40
$MgSO_4$	4.00
$CaSO_4$	4.80
NaCl	2.60

The ion exchange method described above can be used to separate Sb(III) from the matrix in the case of highly contaminated samples (ex: mine impacted pore water). The column procedure will remove the major matrix cations in water (Ca^{+2}, Mg^{+2}, Na^{+}, K^{+}). The procedure removes the majority of Fe(III) as well as Mn, Ge, As and Se. The procedure only works if the initial Fe(III) concentration is below 300 mg/L (Fig. 5).

In the rare case that a strong oxidant besides Fe(III), such as H_2O_2, is present, extra precautions may be required. We have not found dissolved O_2, a natural oxidizing agent, to cause re-oxidation of Sb(III) on a scale of several weeks due to the strength of the reducing agent (KI) and preserving agent (ascorbic acid).

2.11 Rayleigh distillation model

A Rayleigh distillation model is used to describe the isotopic evolution of reactants and products in a closed system starting with all reactant and ending with all products. This model also assumes the reaction is irreversible, with no isotopic interaction between reactants and products. For the reduction of Sb(V) to Sb(III), the δ^{123}Sb of the remaining liquid and the solid product can be modeled using the Rayleigh equation

$$\delta^{123}Sb = (\delta_0 + 1000‰)\left[\frac{c(t)}{c_0}\right]^{\alpha-1} - 1000‰ \qquad (4)$$

Where c_0 and δ_0 are the initial concentration and isotope value of the Sb(V). c(t) is the concentration at time t and α is the isotopic fractionation factor (Eq. 2). The fractionation factor was calculated by minimizing the sum of the squared residuals. The equation for the solid product is:

$$\delta^{123}Sb_{Product} = (\delta^{123}Sb_{Initial} + 1000‰)*[(1-f^{\alpha}) / (1 - f)] - 1000‰ \qquad (5)$$

Where f is $c(t)/c_0$ and α is from Eq. 4.

CHAPTER 3- RESULTS

3.1 Coal ash digests

The coal ash was found to contain 3.57 µg/g Sb; good agreement was obtained between the two digests (3.567 and 3.579 µg/g). The results of δ^{123}Sb analyses of the raw, unprocessed digestate and Sb extracted and purified from the same digest are shown in Table 4. Each solution was analyzed on multiple days. CT2b, CT3b, and CT4b are separate ion exchange separations that had the same quantity of the same digest added to them. Te-doped runs, with initial Te:Sb concentration ratios as high as 0.25, showed no significant offsets from the undoped analyses. No significant differences were observed between results from a raw digest with full matrix and purified Sb extracted from the same digest (Fig. 6).

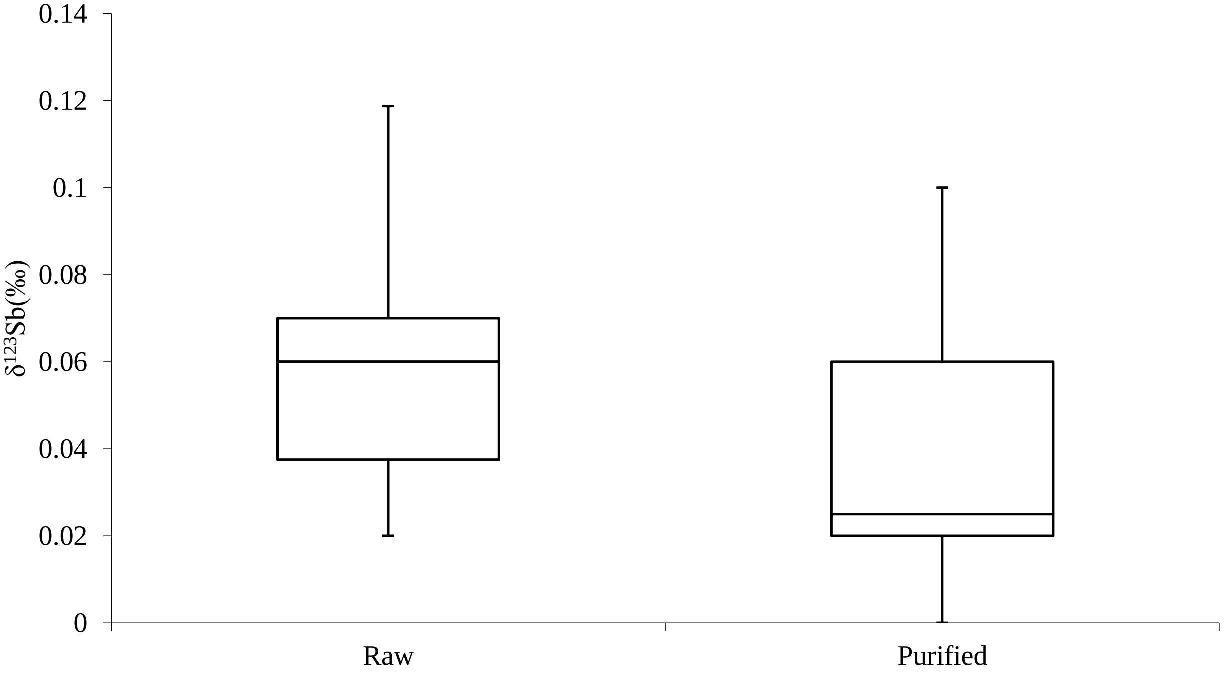

Fig. 6: Boxplot of KFA1 Fly ash with comparison between digests diluted to proper Sb concentration versus samples purified by anion exchange. Boxes indicate 1st and 3rd quartile boundaries; bars indicate minimum and maximum values

Table 4. Results from duplicate analyses of fly ash

Sample name	Date	δ^{123}Sb(‰)	Comment
CT2b	5.28.15	0.03	Purified
CT3b	5.28.15	0.07	Purified
CT4b	5.28.15	0.10	Purified
CT2b	7.23.15	-0.01	Purified
CT3b	7.23.15	0.02	Purified
CT4b	7.23.15	0.02	Purified
Mean 2 Std. Dev.		0.04 ±0.08	
KFA1	4.24.15	0.02	Raw
KFA1	4.24.15	0.06	Raw
KFA1	4.24.15	0.06	Raw
KFA1	5.6.15	0.03	Raw
KFA1	5.6.15	0.05	Raw
KFA1	5.28.15	0.07	Raw
KFA1	5.28.15	0.12	Raw
KFA1	7.23.15	0.10	Raw
KFA1	7.23.15	0.04	Raw
Mean 2 Std. Dev.		0.06 ±0.06	
KFA1 0.125 Te	5.28.15	0.07	Raw, Te added
KFA1 0.1875 Te	5.28.15	0.03	Raw, Te added
KFA1 0.25 Te	5.28.15	0.06	Raw, Te added
Mean 2 Std. Dev.		0.05 ±0.04	
Mean for all analyses 2 Std. Dev.		0.05 ±0.07	

3.2 Equilibrium Isotopic exchange Experiment

The isotopic evolution of Sb(III) and Sb(V) together in solution was followed over the course of many weeks (Fig. 7). The initial concentration ratio of Sb(V) to Sb(III) was slightly above one and appears to have increased by about 25% over the course of the experiment (Table 5). Such an increase could reflect slight oxidation of Sb(III), likely caused by a small amount of residual oxygen in the flask. This may have influenced the δ^{123}Sb values, but only slightly (see discussion). No shifts in the δ^{123}Sb values of the Sb(III) and Sb(V) could be distinguished within the analytical uncertainties after 9 days. A small shift just outside the analytical uncertainty was observed after 80 days. Because isotopic exchange between Sb(III) and Sb(V) in solution would result in greater δ^{123}Sb values for Sb(V) relative to Sb(III), we conclude that after 80 days we observed the first signs that isotopic exchange has occurred.

Table 5. Column recovery and Sb(V):Sb(III) concentration ratio for equilibrium experiment.

Sample No.	Time (days)	Column Recovery	Sb(V):Sb(III)
T0	0	101%	1.15
T1	2	99%	1.20
T2	4	99%	1.18
T3	9	96%	1.33
T4	80	93%	1.53

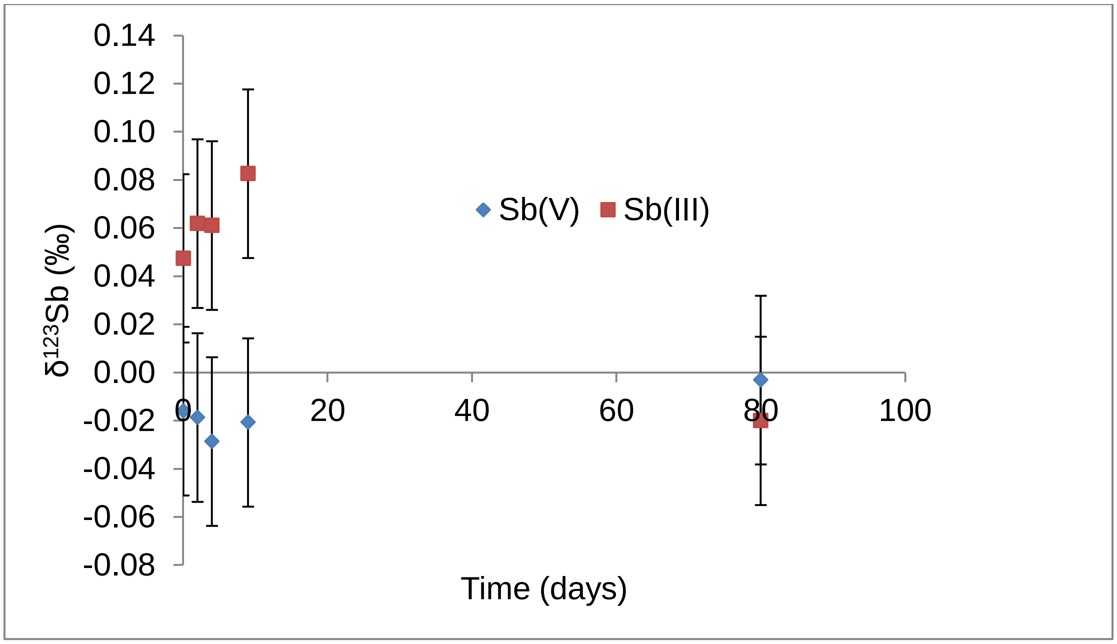

Fig. 7: Measurement of δ^{123}Sb for Sb(V) (blue diamond) and Sb(III) (red square) as a function of time.

3.3 Sulfide reduction experiment

After addition of sulfide to the Sb(V) solutions, no precipitate was observed in the first hours, but within 24 hours orange solids were present. The serum bottles were left in the dark at 20°C for twenty days to allow complete consumption of all sulfide, or in the one experiment with excess sulfide, of Sb. This experiment obtained 99.96% reduction of Sb(V). As a result there was not enough Sb left in solution to obtain an accurate δ^{123}Sb. Results from the other bottles were fit to a Rayleigh distillation model (e.g., Scott et. al. 2004).

The best fit for the Rayleigh model was obtained by maximizing the coefficient of determination for the least squares regression lines. This was calculated as:

$$R^2 = 1-(SS_{residual}/SS_{total}) \qquad (6)$$

Where $SS_{residual}$ is the sum of the squared residuals, $\Sigma_i(y_i - f_i)^2$ and SS_{total} is $\Sigma_i(y_i - \text{mean}(y))^2$. f_i is the model value for a given extent of reaction; y_i is the experimentally measured value. The Rayleigh models values (f) were varied by adjusting α until the closest fit (maximum R^2) for the liquid and solid lines was achieved. We obtained a combined (liquid + solid) R^2 of 0.974 by using an α value of 0.9986 (ε = -1.42‰). A best –fit equilibrium fractionation model was determined via the same fitting method (R^2 = 0.73). Neither model fits all of the data points within the analytical uncertainties. The Rayleigh model deviates slightly (<0.2‰) from 5 out of the 11 measurements. The equilibrium model fits most of data points better than the Rayleigh model, but the last data point of the dissolved Sb series show a very large (1.4‰) deviation from the model. The data are interpreted in more detail in the discussion chapter.

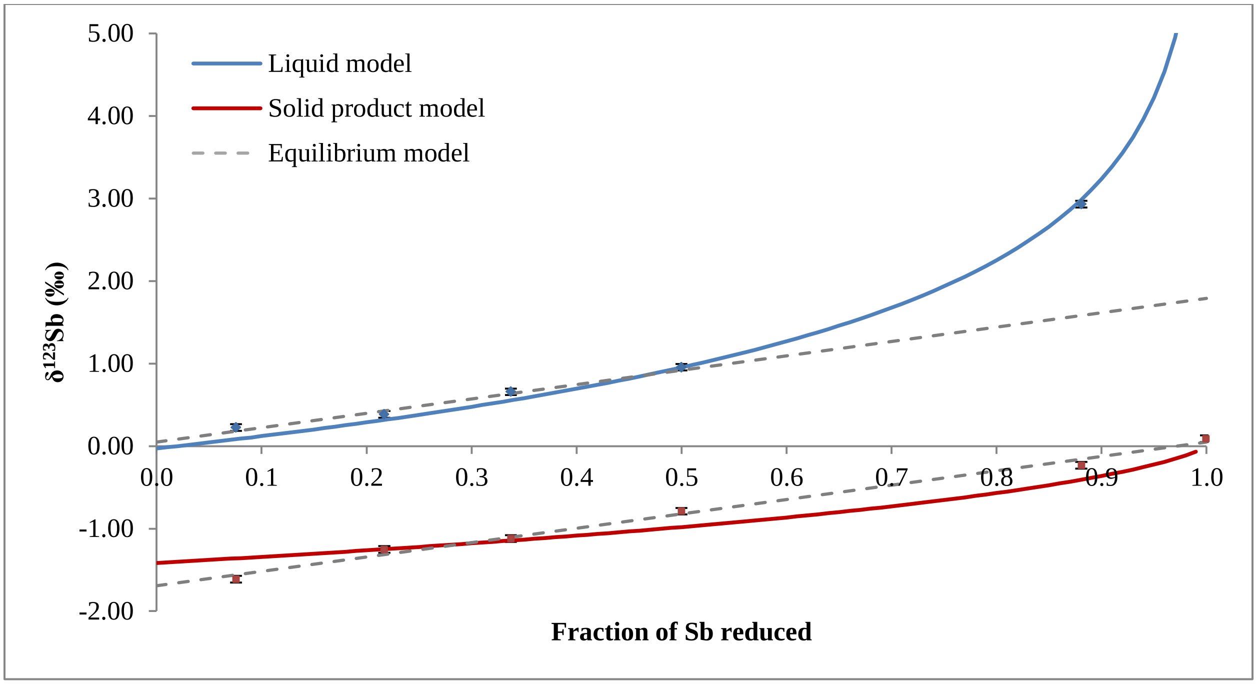

Fig. 8: Results from batch experiments reacting Sb(V)$_{(aq)}$ with sulfide to form $Sb_2S_{3(S)}$. Separate bottles were started with equal masses of Sb(V); the mass of added sulfide varied. δ^{123}Sb (relative to AOA312974) is given for the solid product (red squares) and the remaining Sb in solution (blue diamonds). The best-fit Rayleigh model is shown, with α equal to 0.9986 (ε = -1.42‰). An equilibrium model for both liquid and solid is plotted as a dashed line. Measurement uncertainty is given by the size of the markers.

CHAPTER 4- DISCUSSION

4.1 Isotopic exchange between Sb(III) and Sb(V)

The equilibrium experiment was designed to exclude all chemical processes other than isotopic exchange. However, in the presence of even small amounts of O_2, Sb(III) is prone to oxidation, which could alter δ^{123}Sb. Results to date suggest that a small amount of oxidation may have occurred in the serum bottle (Table 5). We expect that a small amount of residual oxygen at the outset of the experiment caused rapid oxidation of Sb(III) within the first 9 days. More oxidation occurred after 80 days, but the ratio appears to be stabilizing over time as all oxygen is consumed.

Oxidation of Sb(III) during an isotopic exchange experiment between dissolved Sb(III) and dissolved Sb(V) could have three outcomes that depend on whether isotopic fractionation occurs during Sb(III) oxidation. Fractionation during Sb(III) oxidation has not been measured before; the following scenarios describe the hypothetical result if this was known. In the first scenario, there is little fractionation caused by oxidation. In that case, oxidation would have little effect on the results. In the second case, oxidation involves a fractionation with the product being enriched in ^{123}Sb relative to the reactant. In this case, the value of δ^{123}Sb in Sb(III) would decrease and that in Sb(V) would increase. This effect is in the same direction as isotopic exchange (see below) and would not be easily observable. In the third case, oxidation would produce a fractionation with the product Sb(V) having greater ^{121}Sb relative to the reactant. In that case, δ^{123}Sb in the Sb(III) would increase and δ^{123}Sb in the Sb(V) would decrease. In this scenario, because oxidation and isotopic exchange produce opposite effects, it is possible that a small amount of exchange occurred, but was masked by oxidation. However, given that the amount of oxidation was small, the maximum amount of exchange that could have been masked was low.

Isotopic exchange happens through the following reaction:

$^{123}\mathrm{Sb(III)} + {}^{121}\mathrm{Sb(V)} = {}^{121}\mathrm{Sb(III)} + {}^{123}\mathrm{Sb(V)}$ (7)

In this reaction there is an implied transient intermediate step where Sb is present as Sb(IV). The reaction happens by electron transfer during contact between Sb(III) and Sb(V). The exchange happens by one-electron transfer steps: Theory suggests that two-electron transfer is generally very unlikely, and can be significant only if both intermediates do not have stable oxidation states (Linck 1986). Thus, the two-electron transfer isotopic exchange between Sb(III) and Sb(V) is expected to be much slower than exchange between Fe(III) and Fe(II), which is completed with a single electron transfer. The kinetics of isotopic exchange are also inhibited by coordination changes. The need for multiple electron transfer and coordination changes have been invoked as the causes of very slow isotopic exchange observed for U and Cr (Wang et. al. 2015a; Wang et. al. 2015b).

The direction of isotopic equilibrium fractionation can be predicted based on qualitative guidelines outlined by Schauble (2004). The zero point energy (lowest quantum energy state) slightly shifts for different isotopes in equivalent bonds. As a result of this effect, heavy isotopes of an element will usually concentrate in the state where that element forms the stiffest bonds. For Sb, we expect that ^{123}Sb should preferentially partition into the Sb(V) state (products favored in Eq. 7).

The results from our experiment (Fig. 7) indicate no significant change in the δ^{123}Sb of the Sb(V) and a very small change in that of Sb(III) during the first 9 days. The slight shift in the first few Sb(III) data points is only slightly outside the analytical uncertainty. An equal and opposite shift the Sb(V) pool, which must occur given the nearly 1:1 Sb(V):Sb(III) ratio, was not observed. Thus, we conclude that no significant exchange occurred in the first 9 days. After 80 days, it appears that a small amount of isotopic exchange had occurred that was slightly larger than the analytical uncertainty. Because the changes are so close to uncertainty, more data is needed to see if the same trend continues.

At the conditions we performed our experiment (1.0 M HCl), pH was very low and most Sb was in chloride form ($SbCl_3$ and $SbCl_6^-$) with some portion as Sb- hydroxy/chloro complexes (Neumann 1954; Milne 1975). The aqueous speciation of Sb could have an influence on the rate of isotopic exchange. Accordingly, the experiment provides an initial determination of exchange rate but is not directly applicable to natural systems or laboratory experiments with different matrix compositions.

The rate of isotopic exchange depends on Sb concentrations. For a system with high concentrations of Sb(III) and Sb(V), interactions between Sb(III) and Sb(V) atoms would be frequent, and thus isotopic exchange will occur more often. At lower concentrations, Sb(III)-Sb(V) collisions would be relatively rare. Hypothetically, we consider the case where the exchange rate is proportional to the number of Sb(III)-Sb(V) collisions, which should be proportional to [Sb(III)]*[Sb(V)]. In this case, the exchange rate in real systems, with concentrations lower by a factor of 10^5 or more, would be slower by a factor of roughly 10^{10}. Even if the exchange kinetics do not follow this first-order relationship, the rate would be greatly diminished at low concentrations. Slow isotopic exchange at low concentration has been shown by other authors such as for exchange between dissolved Cr(III) and dissolved Cr(VI) (Wang et. al. 2015a). If we assume the first order relationship between Sb concentration and exchange rate and that no isotopic exchange was observed over the month in our experiment, then roughly 80,000 years would be required before isotopic exchange would be a factor to consider, at room temperature.

4.2 Kinetic isotope fractionation during reduction by sulfide

During the course of experimentation we discovered that the liquid fraction from the sulfide reduction experiment contained a significant portion of Sb(III). The liquid portion from 2 different experiment bottles were put through the speciation procedure to separate Sb(III) and Sb(V) immediately after reaction vessels were opened. The liquid phase contained about 25% Sb(III) (Table 6). There are two likely explanations for this: Either some colloidal Sb_2S_3 passed through the 0.22 μM filter and became dissolved in the HCl medium used for the separation, or there was some remaining Sb(III) in solution that did not precipitate as Sb_2S_3.

Table 6. Values from speciation of sulfide reduction experiment liquid portions

Sample ID	Column recovery	Fraction as Sb(III)	δ^{123}Sb Total	δ^{123}Sb Sb(III)	δ^{123}Sb Sb(V)
2L	95%	22%	0.39	-0.61	0.84
5L	92%	24%	2.93	2.1*	3.23

Details from speciation of liquid samples 2 (22% reduction) and 5 (88% reduction). Precision of δ^{123}Sb values are ±0.04‰ (2σ). *This point has a larger uncertainty of ~0.1‰ due to a large drift in mass bias during sample acquisition.

This finding indicates that there are three "phases" present in the reaction vessels: the original aqueous Sb(V), a small portion of mobile Sb(III), and the solid Sb_2S_3. Thus the δ^{123}Sb of the liquid portion originally thought to be pure Sb(V) (Fig. 8) actually represents a combination of original Sb(V) and this "dissolved" Sb(III).

If colloids were present and had passed through the filter, they would decrease the δ^{123}Sb of the liquid portion below the value of the Sb(V) alone. This decrease in δ^{123}Sb would be small in the early stages, when little precipitate has formed and the Sb(V) concentrations was still high. Greater errors would occur at greater extents of reduction, when the precipitate mass was much greater than dissolved Sb(V). The steep increase in δ^{123}Sb at high extents of reaction and lack of deviation from a Rayleigh model argue against this explanation.

Complexity arises because there are two, competing sulfide-consuming reactions in the experiment: (1) the reduction of Sb(V) and (2), the precipitation of Sb_2S_3. If the reduction of Sb(V) proceeds much faster than Sb_2S_3 precipitation, then an intermediate dissolved Sb(III) will build up over time. When all sulfide has been consumed, there will be a remaining Sb(III) "pool" that has not been precipitated. Because I assumed that Sb(III) would be removed from solution, I prepared the liquid phase samples for isotopic analyses without a separation of Sb(III) and Sb(V). I subsequently reduced all Sb(V) with KI before analysis. Accordingly, the reported δ^{123}Sb values are for a mixture of Sb(III) and Sb(V), with their proportions unknown. The δ^{123}Sb values of the Sb(V) fraction must be greater, and the true isotopic fractionation must also be greater than that derived from the Rayleigh model fit.

The applied Rayleigh model to our data has a very good fit, but there are some outliers that do not fit the model. This is especially apparent in the solids, where it appears the data conforms more closely to an equilibrium model (Fig. 8). The experiment is almost certainly not influenced by isotopic exchange for two reasons. First, the liquid portion conforms closely to a kinetic model, and one data point departs very strongly from the equilibrium model. Second, our isotopic exchange rate experiment indicates slow isotopic exchange, and thus equilibrium would not be approached over the 20 days that the experiment was run.

Assuming the isotope fractionation was a kinetic effect, the small differences between the data and the Rayleigh model suggest that the fractionation factor varied between the five bottles used to attain five different extents of reaction (the data are not a single time series). If isotopic fractionation depends on the conditions of the experiment, it is possible that the concentration of sulfide influenced the fractionation. In a reaction which is much more limited in reducing agent, it could create a larger isotope effect which would decrease δ^{123}Sb of the solid. As the concentration of reducing agent increases, this effect is lessened. This hypothesis fits our observation that the first point (very low sulfide) falls below the Rayleigh model and later points (high sulfide) have more positive δ^{123}Sb than predicted. This type of shifting isotope fractionation factor was also postulated by Rashid and Krouse (1985) for Se(IV) reduction.

The observed fractionation in this experiment is what would be expected from mass-dependent fractionation. The kinetic preference of the lighter isotope reacting faster can be explained by noting that a lighter isotope will have a greater zero point energy and is thus more likely to break bonds than a heavier one (Urey 1947). In general it has been observed that the larger the change in bonding, the greater fractionation that occurs. There are significant bond changes during this reaction. The initial Sb(V)- hydroxyl/chloride complex is probably octahedral, similar to $Sb(OH)_6^-$ (Pauling 1933). To a first approximation the solid Sb_2S_3 product should have a similar bond coordination to the mineral stibnite which has trigonal pyramidal and square pyramidal portions (coordination number = 7) (Holleman and Wiberg 2001). ^{121}Sb is preferentially reduced and precipitated indicating a kinetic favorability over ^{123}Sb, based on these bond changes. Similar kinetic isotope trends are observed in many elements including Cr, Te, Fe, and Se.

The magnitude of kinetic isotopic fractionation is often dependent on the mechanism by which the reaction occurs. A better understanding of the mechanism of Sb(V) reduction by sulfide could provide greater insight into our results and be useful in extending results to other studies. The reaction pathway for reduction of dissolved Sb(V) by sulfide to form Sb_2S_3 is quite complex. For simplicity, we will assume the Sb(V) in the system is present as $Sb(OH)_3Cl_3^-$ even though there will be some portion as $Sb(OH)_2Cl_4^-$ and $Sb(OH)_4Cl_2^-$ (Neumann 1954). With the 0.5 M HCl concentration (and low (~50 μM) sulfide) of this experiment, Sb(III) may be found mostly as $SbCl_4^-$ (Milne 1975). The Sb(V) is reduced to aqueous Sb(III) by sulfide in the following reaction:

$4Sb(OH)_3Cl_3^- + HS^- + 4Cl^- + 3H^+ = 4SbCl_4^- + SO_4^{2-} + 8H_2O$ (8)

Sb_2S_3 precipitation is then thought to follow this reaction:

$2SbCl_4^- + 3HS^- = Sb_2S_3 + 3H^+ + 8Cl^-$ (9)

Combining the two gives the overall reaction:

$4Sb(OH)_3Cl_3^- + 7HS^- = 2Sb_2S_3 + 3H^+ + 12Cl^- + SO_4^{2-} + 8H_2O$ (10)

The formation of metastibnite (Sb_2S_3) as an end product of this reaction is supported by previous studies (Polack et. al. 2009; Spycher and Reed 1989). Stability of metastibnite is favored at lower pH (Spycher and Reed 1989). The 0.5 M HCl solvent in this experiment forces strong precipitation of reduced Sb. The final product of oxidized sulfur, listed as sulfate in Eq. 10, is uncertain. Polack et. al. (2009) suggest that S^0 dominates but do not exclude the possible presence of other oxidation products of sulfide.

According to Eq. 10, the stoichiometry should dictate that 2 moles Sb(V) and 3.5 moles sulfide produce 1 mole of Sb_2S_3 meaning perfect stoichiometry needs S:Sb ratio of 1.75. In the first experiment the average ratio of S:Sb of fraction reduced compared to sulfide added, was estimated to be 3.9 ± 0.5 (1 stddev). The difference between the theoretical and observed stoichiometry could be due to the instability of the sulfide solution. Sulfide is very prone to oxidation. Less sulfide added to the experiment than calculated, would artificially increase the measured S:Sb ratio as we have observed.

The fractionation determined from this experiment is only applicable for the conditions of the experiment. Thus the fractionation during Sb(V) reduction by sulfide in nature will be different. However, the magnitude of fractionation is controlled by bond changes, which in natural systems are likely to be similar to this experiment. These results provide insight into the general magnitude of isotopic fractionation that will be observed in real systems.

4.3 Comparison of isotopic fractionation to previous work

I have presented the first experiment to examine the rate of isotopic exchange between Sb(III) and Sb(V) in solution. We cannot obtain a half-life for the system to reach isotopic equilibrium, because not enough isotopic exchange has occurred to date. We would expect similarities in half-life of exchange reaction between Sb and U isotopic equilibrium because both involve transfer of two electrons.

Isotopic fractionation during reduction of Sb(V) to Sb(III) by KI was reported by Rouxel et. al. (2003). Two parallel experiments yielded differing fractionation factors. The first experiment combined a 10 ug/L Sb(V) solution in 0.1% KI while the second had a higher KI concentration (0.5%) and included an added “basalt matrix”. No details of the basalt matrix were provided by the authors, but we assume this involved dissolved ions derived from total digestion of basalt. The time provided for reduction to occur in both experiments was 30 – 60 minutes; a rapid reduction rate. The authors extracted fractionation factors (ε) for the first and second experiments of -0.55‰ and -0.9‰, respectively, after applying Rayleigh models to their data.

Isotopic fractionation in our experiment was much larger (ε = -1.42‰). Kinetic isotope fractionation is typically sensitive to reaction rate, reaction mechanism, the presence of exchange catalysts, and temperature (Schauble 2004). In a faster reaction, the mass-dependent fractionation may be overwhelmed, resulting in smaller fractionation. This concept is known as a “diffusive barrier effect” as described in Kitchen et. al. (2012; and refs. therein). In the experiment of Rouxel et. al. (2003), it is possible that the reactions were diffusion-limited due to the high 0.1 – 0.5% M/V reducing agent concentrations used. This could have led to a muting of isotopic fractionation. In our study, care was taken to avoid rapid reaction; the reaction with sulfide at the lower concentration used in our study takes many hours before solid precipitate appears. It is also possible that the weaker fractionation observed in the Rouxel et al. (2003) experiments reflects large differences in reaction mechanism between KI-driven reduction and sulfide- driven reduction. These comparisons highlight that fractionation factors vary depending on reaction mechanism and other conditions. More work is needed to develop an adequate working knowledge of Sb isotope systematics for use in future studies.

4.4 Applications and future work

This study can be applied in two important, but very distinct types of geochemical studies: modern Sb redox studies associated with contamination and ore applications and paleo-redox studies that seek to constrain past redox conditions using the rock record. The geochemical properties of many metals and metalloids, like Sb, depend on their valence state. As described above, reduced Sb tends to be removed from a system more readily than the oxidized form. Learning more about Sb isotope systematics can provide us with more information about Sb redox in environmental and ore-deposition settings.

The Sb isotope systematics could be useful in better understanding of formation of stibnite and other Sb ore deposits. For example, Sb isotopes might be used to distinguish between the two main Sb deposit types: Carbonate-replacement deposits (Xikuangshan, Hunan Province, China) and gold-Sb epithermal deposits (Carlin type) (Wintzer and Guberman, 2015). If the two deposit types have different isotopic signatures, it could provide information on the ore formation and could potentially be useful in determining gold-rich Sb deposits.

In regards to Sb isotopes as redox indicators in environmental applications, the sulfide-driven Sb(V) reduction experiment provides us with an initial indication of the magnitude of fractionation induced by the reaction, but more work is needed. We have observed that isotopic fractionation during reduction of Sb(V) by sulfide is much larger than that observed in a previous study using KI, a reductant that is rare in nature. In order to make more informed interpretations of field Sb isotope studies, more laboratory experiments are needed to explore Sb isotopic fractionation during (1) microbial redox reactions, (2) oxidation of Sb(III) to Sb(V) by O_2, (3) adsorption onto Fe, Al and Mn compounds and (4) reduction by Fe(II)-bearing phases.

Emerging studies have revealed that microbes play a large role in the oxidation state of Sb. It is thought that the presence of Sb in nature in its less thermodynamically stable oxidation state (Sb(III) in surface water and/or Sb(V) in anoxic water) is attributed to microbial transformation; however strong evidence has not been provided (Filella et. al. 2002). On the other hand, there is strong evidence that certain microbes can grow through reduction or oxidation of Sb (Lyalikova 1974; Abin and Hollibaugh 2013; Kulp et. al. 2013). One important discovery was the observed ability of a microbe capable of reducing aqueous Sb(V) and forming solid Sb_2O_3 (Abin and Hollibaugh 2013). In the future it will be essential to measure Sb isotopic fractionation induced by microorganisms.

In a similar vein of isotope geochemistry applications but vastly different purpose compared to environmental studies, is the field of paleo-redox. Sb isotope measurements within segments of the rock record can be used to make interpretations on the rise and fall of atmospheric O_2. This isotopic approach to paleo-redox has been applied to many elements, like Cr, S, Mo and U (e.g., Frei et al. 2009; Archer and Vance 2008; Lyons et. al. 2014; Kendall et. al. 2013). For example, Frei et al. (2009) analyzed δ^{53}Cr of numerous Precambrian BIFs and used these data to suggest that the Great Oxidation Event did not lead to a stepwise increase in atmospheric oxygen but instead was followed by large fluctuations over the next billion years.

Because the mobility of Sb is partly controlled by valence state, changing oxidation states in the past would either mobilize or precipitate Sb. Because isotopes can be used to track Sb redox, they could be used in conjunction with other methods to determine past redox conditions. The estimated Sb residence time in the modern oceans is long (~5,700 years) relative to the ~1,000 year mixing time of the oceans (Broecker and Peng 1982). As such, the marine Sb isotope record could be a good candidate as a redox proxy for the global ocean.

CHAPTER 5– CONCLUSIONS

In this study we have obtained greater insight into certain analytical procedures needed for Sb isotope analysis and have performed some of the first environmentally relevant Sb isotope fractionation experiments. We have investigated the efficacy of Sb speciation analysis by anion exchange resin in more detail than earlier studies. Quantitative Sb recovery is obtained with this method and while aliquots of eluent may be artificially fractionated, no overall artificial fractionation is induced if column recovery is near 100%. HG-MC-ICP-MS is effective at measuring isotopic variations in natural samples. HG is shown to be an effective filter so that matrix effects do not cause interference in most cases. The pre-reducing solution has been observed to greatly reduce the isobaric interference from ^{123}Te, via Te(IV) reduction to solid Te^0. Tellurium is generally rare in natural waters, but in the event that larger concentration exists, a correction based on measurement of ^{126}Te can be applied to correct measured ^{123}Sb/^{121}Sb ratios.

We have shown that isotopic exchange between Sb(V) and Sb(III) in solution is not significant over experiment duration scales of weeks. These results are similar to those obtained for other isotopic systems such as Cr and U (Wang et. al. 2015a; Wang et. al. 2015b). This result is important because the rate at which a system reaches isotopic equilibrium could have an impact on how kinetic isotope experiments are interpreted. This is beneficial for dynamic natural water systems. In most natural settings, water flow is fast enough such that the system will not measurably progress toward isotopic equilibrium. Instead, any observed variations in δ^{123}Sb can be attributed to other processes such as reduction or adsorption.

We observed significant fractionation during the reduction of aqueous Sb(V) by sulfide to form solid Sb_2S_3. Sb reduction has previously been shown to fractionate isotopes as ^{121}Sb is preferentially reduced while remaining Sb(V) is enriched in ^{123}Sb (Rouxel et. a. 2003). We observed significantly larger fractionation, expressed as ε, of -1.42‰ compared to Rouxel et. al. (2003) which observed a maximum fractionation of -0.9‰ by a potassium iodide reducing agent. This difference may be attributed to slower reaction kinetics in our experiments or to contrasting reaction mechanisms for sulfide-driven reduction compared to KI-driven reduction.

Future work needed for expanding understanding Sb isotope geochemistry includes (i) more detailed isotopic exchange studies including solid-liquid equilibria; (ii) fractionation as Sb adsorbs onto various solid media; (iii) fractionation as Sb oxidizes and dissolves; and perhaps most importantly (iv) extent of influence by microbial redox reactions. There are many opportunities for studies that will help to develop understanding of Sb isotope systematics and then apply Sb isotope measurements toward a better understanding of Sb geochemistry in modern and ancient environments.

CHAPTER 6- REFERENCES

Abin, C; Hollibaugh, J. Dissimilatory Antimonate Reduction and Production of Antimony Trioxide Microcrystals by a Novel Microorganism. *Environmental Science & Technology*. **2014**, (48), 681-688.

Archer, C; Vance, D. The isotopic signature of the global riverine molybdenum flux and anoxia in the ancient oceans. *Nature Geoscience*. **2008**, *1*(9), 597-600.

Amarasiriwardena, D; Wu, F. Antimony: emerging toxic contaminant in the environment. *Microchemical Journal*. **2011**, *97*(1), 1-3.

Anbar, AD; Roe, JE; Barling, J; Nealson, KH. Nonbiological fractionation of iron isotopes. *Science*. **2000**, *288*(5463), 126-128.

Anderson, CG. The metallurgy of antimony. *Chemie der Erde-Geochemistry*. **2012**, 72, 3-8.

Araki, Y; Tanimizu, M; Takahashi, Y. Antimony isotopic fractionation during adsorption on ferrihydrite. *Geochim. Cosmochim. Acta*. **2009**, 73, A49.

Asaoka, S; Takahashi, Y; Araki, Y; Tanimizu, M. Preconcentration method of antimony using modified thiol cotton fiber for isotopic analyses of antimony in natural samples. *Analytical Sciences*. 2011, 27(1), 25-28.

Berglund, M; Wieser, ME. Isotopic compositions of the elements 2009 (IUPAC Technical Report). *Pure and Applied Chemistry*. **2011**, *83*(2), 397-410.

Berna, EC; Johnson, TM; Makdisi, RS; Basu, A. Cr stable isotopes as indicators of Cr (VI) reduction in groundwater: a detailed time-series study of a point-source plume. *Environmental science & technology*. **2009**, 44(3), 1043-1048.

Buschmann, J; Canonica, S; Sigg, L. Photoinduced oxidation of antimony (III) in the presence of humic acid. *Environmental science & technology*. **2005**, *39*(14), 5335-5341.

Broecker, WS; Peng, TH. Tracers in the Sea. *Lamont-Doherty Geol. Obs., Palisades, NY*. **1982**, 690 pp.

Dedina, J; Tsalev, DL. Hydride Generation Atomic Absorption Spectrometry. Wiley, Chichester, NY. **1995**, 526.

Filella, M; Belzile, N; Chen, YW. Antimony in the environment: a review focused on natural waters. I. Occurrence. *Earth-Sci. Rev*. **2002**, 57, 125-176.

Frei R; Gaucher C; Poulton SW; Canfield DE. Fluctuations in Precambrian atmospheric oxygenation recorded by chromium isotopes. *Nature* . **2009**, 461, 250–254.

Guo, X; Wu, Z; He, M. Removal of antimony (V) and antimony (III) from drinking water by coagulation–flocculation–sedimentation (CFS). *Water research*. **2009**, 43, 4327-35.

Hall, GE; Pelchat, JC. Analysis of geological materials for bismuth, antimony, selenium and tellurium by continuous flow hydride generation inductively coupled plasma mass spectrometry. *Journal of Analytical Atomic Spectrometry*. **1997**, 12(1), 97-102.

He, M; Wang, X; Wu, F; Fu, Z. Antimony pollution in China. *Science of the total environment*. **2012**, *421*, 41-50.

Holleman, A. F.; Wiberg, E. *Inorganic Chemistry,* San Diego: Academic Press. **2001**, 765-766

Ilgen, AG; Trainor, TP. Sb (III) and Sb (V) sorption onto Al-rich phases: hydrous Al oxide and the clay minerals kaolinite KGa-1b and oxidized and reduced nontronite NAu-1. *Environmental science & technology*. **2011**, *46*(2), 843-851.

Johnson, CM; Skulan, JL; Beard, BL; Sun, H; Nealson, KH; Braterman, PS. Isotopic fractionation between Fe (III) and Fe (II) in aqueous solutions. *Earth and Planetary Science Letters*. **2002**, *195*(1), 141-153.

Johnson, TM. Stable isotopes of Cr and Se as tracers of redox processes in earth surface environments. In *Handbook of environmental isotope geochemistry*. 2012, 155-175. Springer Berlin Heidelberg.

Kendall, B; Brennecka, GA; Weyer, S; Anbar, AD. Uranium isotope fractionation suggests oxidative uranium mobilization at 2.50Ga. *Chemical Geology*. **2013**, *362*, 105–114.

Kitchen, JW; Johnson, TM; Bullen, TD; Zhu, J; Raddatz, A. Chromium isotope fractionation factors for reduction of Cr (VI) by aqueous Fe (II) and organic molecules. *Geochimica et Cosmochimica Acta*. **2012**, *89*, 190-201.

Kulp, TR; Miller, LG; Braiotta, F; Webb, SM; Kocar, BD; Blum, JS; Oremland, RS. Microbiological reduction of Sb (V) in anoxic freshwater sediments. *Environmental science & technology*. **2013**, *48*(1), 218-226.

Leuz, AK; Johnson, CA. Oxidation of Sb (III) to Sb (V) by O 2 and H 2 O 2 in aqueous solutions. *Geochimica et Cosmochimica Acta*. **2005**, *69*(5), 1165-1172.

Leuz, AK; Mönch, H; Johnson, CA. Sorption of Sb (III) and Sb (V) to goethite: influence on Sb (III) oxidation and mobilization. *Environmental science & technology*. **2006**, *40*(23), 7277-7282.

Linck RG. Electron-transfer and electrochemical reactions. Photochemical and other energized reactions. In *Inorganic Reactions and Methods*. **1986**, 15, 16

Lobo, L; Devulder, V; Degryse, P; Vanhaecke, F. Investigation of natural isotopic variation of Sb in stibnite ores via multi-collector ICP-mass spectrometry–perspectives for Sb isotopic analysis of Roman glass. *Journal of Analytical Atomic Spectrometry*. **2012**, 27(8), 1304-10.

Lobo, L; Degryse, P; Shortland, A; Vanhaecke, F. Isotopic analysis of antimony using multi-collector ICP-mass spectrometry for provenance determination of Roman glass. *Journal of Analytical Atomic Spectrometry*. **2013**, *28*(8), 1213-1219.

Lobo, L; Degryse, P; Shortland, A; Eremin, K; Vanhaecke, F. Copper and antimony isotopic analysis via multi-collector ICP-mass spectrometry for provenancing ancient glass. *Journal of Analytical Atomic Spectrometry*. **2014**, *29*(1), 58-64.

Łukaszczyk, L; Żyrnicki, W. Speciation analysis of Sb (III) and Sb (V) in antileishmaniotic drug using Dowex 1× 4 resin from hydrochloric acid solution. *Journal of pharmaceutical and biomedical analysis*. **2010**, 52(5), 747-751.

Lyalikova, NN. *Stibiobacter senarmontii* - a new microorganism oxidizing antimony. *Mikrobiologiia*. **1974**, *43*(6), 941.

Lyons, TW; Reinhard, CT; Planavsky, NJ. The rise of oxygen in Earth/'s early ocean and atmosphere. *Nature*. **2014**, *506*(7488), 307-315.

Milne, J. Spectrophotometric studies on Sb (III) in hydrochloric acid solutions. *Canadian Journal of Chemistry*. **1975**, *53*(6), 888-893.

Näykki, T; Perämäki, P; Kujala, J; Mikkonen, A. Optimization of a flow injection hydride generation atomic absorption spectrometric method for the determination of arsenic, antimony and selenium in iron chloride/sulfate-based water treatment chemical. *Analytica chimica acta*. **2001**, *439*(2), 229-238.

Neumann, HM. Antimony (V) Species in Hydrochloric Acid Solution. *Journal of the American Chemical Society*. **1954**, *76*(10), 2611-2615.

Pauling, L. The formulas of antimonic acid and the antimonates.*Journal of the American Chemical Society*. **1933**, *55*(5), 1895-1900.

Pilarski, J; Waller, P; Pickering, W. Sorption of antimony species by humic acid. *Water, air, and soil pollution*. **1995**, *84*(1-2), 51-59.

Poon, R; Chu, I; Lecavalier, P; Valli, VE; Foster, W; Gupta, S; Thomas, B. Effects of antimony on rats following 90-day exposure via drinking water. *Food and Chemical Toxicology*. **1998**, *36*(1), 21-35.

Polack, R; Chen, YW; Belzile, N. Behaviour of Sb (V) in the presence of dissolved sulfide under controlled anoxic aqueous conditions.*Chemical Geology*. **2009**, *262*(3), 179-185.

Rashid, K; Krouse, HR. Selenium isotopic fractionation during reduction to Se0 and H2Se. *Canadian journal of chemistry*. **1985**, *63*(11), 3195-3199.

Resongles, E; Freydier, R; Casiot, C; Viers, J; Chmeleff, J; Elbaz-Poulichet, F. Antimony isotopic composition in river waters affected by ancient mining activity. *Talanta*. **2015**, *144*, 851-861.

Ritchie, VJ; Ilgen, AG; Mueller, SH; Trainor, TP; Goldfarb, RJ. Mobility and chemical fate of antimony and arsenic in historic mining environments of the Kantishna Hills district, Denali National Park and Preserve, Alaska. *Chemical Geology*. **2013**, *335*, 172-188.

Rouxel, O; Ludden, J; Carignan, J; Marin, L; Fouquet, Y. Natural variations of Se isotopic composition determined by hydride generation multiple collector inductively coupled plasma mass spectrometry. *Geochimica et Cosmochimica Acta*. **2002**, 66(18), 3191-3199.

Rouxel, O; Ludden, J; Fouquet, Y. Antimony isotope variations in natural systems and implications for their use as geochemical tracers. *Chemical Geology*. **2003**, 200, 25-40.

Schauble, EA. Applying stable isotope fractionation theory to new systems. *Reviews in Mineralogy and Geochemistry*. **2004**, 55(1), 65-111.

Scott, KM; Lu, X; Cavanaugh, CM; Liu, JS. Optimal methods for estimating kinetic isotope effects from different forms of the Rayleigh distillation equation. *Geochimica et Cosmochimica Acta*. **2004**, *68*(3), 433-442.

Shotyk, W; Krachler, M; Chen, B. Antimony: global environmental contaminant. *Journal of environmental monitoring*. **2005a**, 7(12), 1135.

Shotyk, W; Krachler, M; Chen, B. Anthropogenic impacts on the biogeochemistry and cycling of antimony. *Metal ions in biological systems*. **2005b**, *44*, 171.

Smedley, PL; Kinniburgh, DG. A review of the source, behaviour and distribution of arsenic in natural waters. *Applied geochemistry*. **2002**, *17*(5), 517-568.

Spycher, NF; Reed, MH. As (III) and Sb (III) sulfide complexes: an evaluation of stoichiometry and stability from existing experimental data.*Geochimica et Cosmochimica Acta*. **1989**, *53*(9), 2185-2194.

Takeno, N. Atlas of Eh-pH diagrams Intercomparison of thermodynamic databases; National Institute of Advanced Industrial Science and Technology (AIST): Tsukuba, Japan. **2005**.

Tanimizu, M; Araki, Y; Asaoka, S; Takahashi, Y. Determination of natural isotopic variation in antimony using inductively coupled plasma mass spectrometry for an uncertainty estimation of the standard atomic weight of antimony. *Geochemical Journal*. **2011**, 45, 27-32.

Thanabalasingam, P; Pickering, WF. Specific sorption of antimony (III) by the hydrous oxides of Mn, Fe, and Al. *Water, Air, and Soil Pollution*. **1990**, *49*(1-2), 175-185.

Ungureanu, G; Santos, S; Boaventura, R; Botelho, C. Arsenic and antimony in water and wastewater: Overview of removal techniques with special reference to latest advances in adsorption. *Journal of environmental management*. **2015**, 151, 326-42.

Urey, HC. The thermodynamic properties of isotopic substances. *Journal of the Chemical Society (Resumed)*. **1947**, 562-581.

Wang, H; Chen, F; Mu, S; Zhang, D; Pan, X; Lee, DJ; Chang, JS. Removal of antimony (Sb (V)) from Sb mine drainage: Biological sulfate reduction and sulfide oxidation–precipitation. *Bioresource technology*. **2013**,146, 799-802.

Wang, X; Johnson, TM; Ellis, AS. Equilibrium isotopic fractionation and isotopic exchange kinetics between Cr (III) and Cr (VI).*Geochimica et Cosmochimica Acta*. **2015a**, *153*, 72-90.

Wang, X; Johnson, TM; Lundstrom, CC. Low temperature equilibrium isotope fractionation and isotope exchange kinetics between U (IV) and U (VI). *Geochimica et Cosmochimica Acta*. **2015b**, *158*, 262-275.

Wiederhold, JG. Metal stable isotope signatures as tracers in environmental geochemistry. *Environmental science & technology*. **2015**, *49*(5), 2606-2624.

Wilson, N; Webster-Brown, J; Brown, K. The behaviour of antimony released from surface geothermal features in New Zealand. *Journal of Volcanology and Geothermal Research*. **2012**, 247, 158-167.

Wintzer, NE; Guberman, DE. Antimony—A Flame Fighter. *U.S. Geological Survey*. **2015**. DOI:10.3133/fs20153021